UNIVERSITÄT BIELEFELD

Faculty of Business Administration and Economics

Working Papers in Economics and Management

No. 09-2023
December 2023

Non-smooth climate change and emergent novel equilibria in an environmental-economic system

Anton Bondarev Alfred Greiner

Bielefeld University
P.O. Box 10 01 31
33501 Bielefeld – Germany

ISSN 2196-2723

→ www.wiwi.uni-bielefeld.de

Non-smooth climate change and emergent novel equilibria in an environmental-economic system

Anton Bondarev* Alfred Greiner†

Abstract

In this paper we study a basic model of economic growth where we integrate a zero-dimensional energy balance model of the Earth. The albedo of the Earth is the piecewise smooth function of the average surface temperature, thus, taking into account possible feedback effects of a higher temperature. The analysis of the model shows that the model with a jump in the albedo has either a unique regular steady-state or two regular steady-states. When the albedo is described by a piece-wise linear function there exists a non-degenerate pseudo-equilibrium where the temperature stabilizes at the upper switching point of albedo increase with a strictly positive level of consumption.

Keywords: Piece-wise smooth system, climate change, optimal control

JEL classification: Q54, C61, O41

*International Business School Suzhou, Xi'an Jiaotong-Liverpool University, Ren'ai Road, 111, 215123 Suzhou, P.R. China. e-mail: anton.bondarev@xjtlu.edu.cn

†Department of Business Administration and Economics, Bielefeld University, Universitaetsstrasse 25, 33615 Bielefeld, Germany. e-mail:agreiner@uni-bielefeld.de

1 Introduction

With the beginning of the industrialization in the late 19th century, the concentration of greenhouse gases (GHGs), such as carbon dioxide, CO_2, methane, CH_4, and nitrous oxide, N_2O in the atmosphere has been continuously rising. For example, global CO_2 increased from about 336 parts per million (ppm) in January 1979, the start of the atmospheric measurement, to about 418 ppm in July 2023, CH_4 rose from 1625 parts per billion (ppb) in July 1984 to 1917 ppb in June 2023 and N_2O went up from in 316 ppb in January 2001 to 337 ppb in June 2023. A higher GHG concentration in the atmosphere raises radiative forcing, where the relationship is characterized by a strictly concave function. For CO_2 it is given by the natural logarithm of that GHG relative to the pre-industrial level, for CH_4 and N_2O by the square root and those GHGs can be converted into CO_2 equivalents, see Greiner and Semmler (2008) p. 61, and for more details the natural science literature cited there.[1] The increase in radiative forcing leads to a higher average global temperature on earth and may generate more extreme weather events.

However, it must be pointed out that the climate of the earth is an extremely complex system and there exist great uncertainties regarding the effects of GHGs, see e.g. the discussion in Greiner et al. (2023) so that one should be careful when using the outcome of climate models for policy recommendations. Despite high model uncertainties with respect to the climate on the Earth, changes in the climatic conditions are likely to influence the economic system of societies. For example, more extreme weather events can cause economic damages and require resources that cannot be used for consumption and/or for investment, although it must be noted that the empirical evidence for more extreme events is small, with the exception of heatwaves (see Ranasinghe et al. (2021), p. 1856, table 12.12, column 3, Alimonti and Mariani (2023), and similar Lomborg (2020)). Nevertheless, with an ongoing increase of the GHG concentration, abrupt changes in the climate system of the Earth cannot be excluded once a certain threshold is exceeded, sometimes referred to as tipping points. In the last IPCC report such tipping points are considered as low-likelihood high-impact outcomes, see Chen et al. (2021) chapter 1.4.4.

[1] Etminan et al. (2016) show that for very high values of GHGs, the relation changes. But, the basic form remains the same, i.e. for CO_2 it is given by the ln and for N_2O and CH_4 by the square root.

Components that are susceptible to tipping points are for example the Arctic Winter Sea Ice, the Antarctic Sea Ice or the Atlantic meridional overturning circulation (AMOC), of which the Gulf Stream is one component (for the complete list, see Lee et al. (2021), table 4.10, p. 634). A weakening of the Gulf Stream (cf. Piecuch and Beal (2023)) could have strong effects on the climate in Europe. Technically, such tipping points can arise when non-linearities or piecewise smooth functions are present in the differential equations describing the evolution of the system. In a simple climate system a piecewise smooth function may occur when the albedo of the earth, determining how much of the incoming energy is reflected to space, is not a constant, but, a function of time, as suggested by Henderson-Sellers and McGuffie (1987) and Schmitz (1991) for example. There, it is posited that the albedo declines as a result of a higher average surface temperature because of feedback effects, such as the melting of glaciers. Those authors suggest that the albedo is a constant up to a certain value and, then, jumps to a lower value once a certain threshold of the temperature is passed or that the albedo is constant, declines linearly when a threshold is reached and becomes constant again, when a second threshold is passed, with the function being non-smooth at the thresholds.

In Greiner and Semmler (2005) a simple model of economic growth was presented that allowed for a zero-dimensional climate module with a state dependent albedo. However, the albedo was modelled as a smooth function of the temperature, thus, avoiding problems resulting from discontinuous and piecewise-smooth functions. It turned out that the competitive market economy is characterized by multiple equlibria and, once a certain thershold is passed, the economy converges to the equilibrium with the higher temperature. The social optimum is characterized by a unique equilibrium unless the damages associated with global warming are extremely small. In this paper we take the model by Greiner and Semmler (2005) as a starting point (referred to as the benchmark model later on in the text), but, posit that the albedo of the Earth is a non-smooth but a piecewise-smooth function of the temperature, respectively, as suggested by Henderson-Sellers and McGuffie (1987) and Schmitz (1991). To analyze the model we proceed as in Bondarev and Upmann (2022) and apply methods known recently from hybrid control systems and from the theory of piecewise-smooth systems (PWS) to the problem of climate change.

In the rest of the paper we proceed as follows. In section 2 we present the structure of the benchmark model by Greiner and Semmler (2005) and in section 3 we give some basic definitions that are necessary for our analysis. Sections 4 and 5 analyze the model with a discontinuous and piecewise linear albedo, respectively, and section 6, finally, concludes.

2 The model

We start with the competitive economy of the benchmark model. The model is a basic endogenous growth model with positive externalities of capital giving rise to ongoing growth. Further, the use of capital in production goes along with GHG emissions that can be reduced by abatement activities. The latter are performed by the representative agent who has to pay taxes on GHG emissions that give an incentive to invest in abatement. The model is fully described by the triple of differential equations (eqs. (21)-(23) in the benchmark paper):

$$\dot{T}(t) = \left(\frac{1367.5}{4}(1-\alpha_1(T)) - 0.95(5.67\times 10^{-8})\frac{21}{109}T^4\right)c_h^{-1} + \left((1-\xi)6.3\ln\frac{M}{M_0}\right)c_h^{-1} \tag{1a}$$

In this, $\dot{T}(t)$ is the zero dimensional climate module describing the temperature increase. The first term in that equation gives the shortwave radiative flux coming from the sun, the second term is the net longwave radiation emitted to space and the third term, finally, represents the radiative forcing due to the GHG concentration M exceeding its pre-industrial level M_0. The GHG concentration evolves according to,

$$\dot{M} = \beta_1\left(\frac{\tau_E}{LK}\right)^{-\gamma/(1+\gamma)} a^{\gamma/(1+\gamma)}\gamma^{-\gamma/(1+\gamma)} - \mu M, \tag{1b}$$

where the first term gives net emissions after abatement which is a function of the tax on GHG emissions, τ_E, the private sector has to pay. The economic dimension of the model is obtained from a standard inter-temporal optimization problem as

$$\dot{c} = c\left((n-\rho) - (1-\alpha)(1-\tau)BD(\cdot) + \left(\frac{\tau_E}{LK}\right)^{1/(1+\gamma)} a^{\gamma/(1+\gamma)}\gamma^{-\gamma/(1+\gamma)} + c\right) \tag{1c}$$

with $c = C/K$ per capita consumption. Initial conditions on the environment, $T(0) = T_0, M(0) = M_0$, are fixed and the consumption path can be chosen freely ($c(0)$ is free).

Function $D(\cdot)$ is the *damage function* and is assumed again the same as in the benchmark model:

$$D(\cdot) := (a_1(T - T_0)^2 + 1)^{-\psi} \tag{1d}$$

We stick to the same calibrated parameter values as in the benchmark model as well as to naming conventions of variables and parameters (see Table 1):

Parameter	Name	Value
ρ	discount rate	0.03
n	population growth rate	0.02
δ	capital depreciation	0.075
M_0	pre-industrial GHG	1
c_h	heat capacity	0.1497
ξ	ocean temperature absorption	0.23
β_1	emissions absorbed by ocean	0.49
μ	inverse of atmospheric lifetime of GHG	0.1
τ	income tax rate	0.15
α	capital share	0.45
B	social return to capital	0.35
$\frac{\tau_E}{LK}$	emission tax rate per capital	0.001
γ	pollution elasticity	1
a	pollution parameter linear sensitivity	$1.65 \cdot 10^{-4}$
a_1	damage function linear sensitivity	0.04
ψ	non-linear damage parameter	0.05

Further details on the choice of these values can be found in the benchmark paper.

The core contribution is in a different approach to modelling the albedo function $\alpha_1(T)$. In the benchmark model the S-shaped smooth function was used as an approximation of the non-smooth albedo changes. Using recent advances in non-smooth control we replace that with two different non-smooth versions. Namely, we first posit that the albedo function has a single jump at some crucial temperature level T_s (Section 4) and next advance to a more realistic scenario of the albedo having a period of linear increase as proposed by e.g. Henderson-Sellers and McGuffie (1987) in Section 5.

To make the paper more self-contained and readable, we first introduce several ideas from the PWS theory and hybrid control theory (a more detailed version can be found in Bondarev and Upmann (2022)).

3 Some definitions

To start with we give some necessary definitions.

3.1 Piecewise-smooth systems

First, we define a piecewise-smooth dynamic system. The differential equation we consider is given by

$$\dot{\mathbf{x}} = \begin{cases} f_-(\mathbf{x}), & \text{if } \alpha(\mathbf{x}) < 0, \\ f_+(\mathbf{x}), & \text{if } \alpha(\mathbf{x}) > 0, \end{cases} \tag{2}$$

with $f_-(\mathbf{x}) \neq f_+(\mathbf{x})$ and $\alpha(\mathbf{x})$ being the switching condition. As α only depends on $\mathbf{x}$, and not on t, we limit ourselves to a *state-driven switch*. In this case, the switching manifold is given by $\Sigma := \{\mathbf{x} \in \mathbb{R}^n : \alpha(\mathbf{x}) = 0\}$, and we henceforth denote the generic element of Σ by $\mathbf{x}_s$. We refer to the vector fields $f_-(\mathbf{x})$ and $f_+(\mathbf{x})$ as the *lower* and the *upper* flow, and denote the (generic) steady-states of f_- and f_+ by $\bar{x}_-$ and $\bar{x}_+$, respectively. Either of f_- and f_+ may have a unique or multiple steady-states; these steady-states can be classified as follows (see Di Bernardo et al., 2008):

Definition 1. *A steady-state $\bar{x}_+$ of an upper flow is called* regular *if $\alpha(\bar{x}_+) > 0$,* virtual *if $\alpha(\bar{x}_+) < 0$, and* boundary *if $\alpha(\bar{x}_+) = 0$. Similarly, a steady-state $\bar{x}_-$ of a lower flow is called* regular *if $\alpha(\bar{x}_-) < 0$,* virtual *if $\alpha(\bar{x}_-) > 0$, and* boundary *if $\alpha(\bar{x}_-) = 0$.*

We henceforth denote by $\mathcal{L}_f \alpha \equiv \langle f, \nabla\alpha \rangle$ the Lie derivative of α along the vector field f. The topology of the switching manifold Σ consists of three types of regions see, *e. g.*(Jacquemard et al., 2013):

Definition 2. *The disjoint subsets of the switching manifold $\Sigma_{CR}, \Sigma_{ES}, \Sigma_{SL} \subset \Sigma$, with $\Sigma_{CR} \cup \Sigma_{ES} \cup \Sigma_{SL} = \Sigma$, are called:*

- crossing region*:* $\Sigma_{CR} := \{\mathbf{x} \in \Sigma : (\mathcal{L}_{f_+}\alpha)(\mathbf{x})(\mathcal{L}_{f_-}\alpha)(\mathbf{x}) > 0\}$*, where the trajectory may cross the switching manifold from one vector field to the other;*

- escaping region*:* $\Sigma_{ES} := \{\mathbf{x} \in \Sigma : (\mathcal{L}_{f_+}\alpha)(\mathbf{x}) > 0, (\mathcal{L}_{f_-}\alpha)(\mathbf{x}) < 0\}$*, where both vector fields are bounced off the switching manifold;*

- sliding region*:* $\Sigma_{SL} := \{\mathbf{x} \in \Sigma : (\mathcal{L}_{f_+}\alpha)(\mathbf{x}) < 0, (\mathcal{L}_{f_-}\alpha)(\mathbf{x}) > 0\}$*, where both vector fields point into the switching manifold.*

When f_- and f_+ have opposite directions at Σ (escaping region and sliding region), there exists a solution that lies on the switching manifold and satisfies $\dot{\mathbf{x}} = f_s(\mathbf{x})$ where f_s is a *sliding flow (sliding vector field)*:

Definition 3. *Let* $\Sigma_{SL}, \Sigma_{ES} \neq \emptyset$*. The PWS system* (2) *possesses* extended Filippov's form*:*

$$\dot{\mathbf{x}} = \begin{cases} f_-(\mathbf{x}) & \text{if } \alpha(\mathbf{x},t) < 0, \\ f_s(\mathbf{x}) & \text{if } \alpha(\mathbf{x},t) = 0, \\ f_+(\mathbf{x}) & \text{if } \alpha(\mathbf{x},t) > 0, \end{cases} \tag{3}$$

with

$$f_s := f_- + \frac{\mathcal{L}_{f_-}\alpha}{\mathcal{L}_{f_-}\alpha - \mathcal{L}_{f_+}\alpha}(f_+ - f_-). \tag{4}$$

being Filippov's sliding flow *(or simply* Filippov's flow*, see Colombo and Jeffrey, 2011).*

The Filippov flow possesses its own steady-states:

$$\bar{x}_s : \ f_s(\bar{x}_s) = 0, \tag{5}$$

which is referred to as a *pseudo-equilibrium* of the PWS system (2). If $(\mathcal{L}_{f_\pm}\alpha)(\mathbf{x}) = 0$, the vector field $f_\pm$ is *tangent* to the switching manifold Σ. Typically these tangency lines (or points) represent boundaries between the crossing, escaping and sliding regions.[2]

[2]Some authors include these boundaries into definition of the sliding or the escaping region, see Tang et al. (2012).

3.2 Hybrid control

Once the dynamics of the state variable in a control problem has the form of (2), the optimal control can no longer be obtained via conventional Maximum Principle. Instead we have several (at least) distinct cases (see Boltyanski (2004), Shaikh and Caines (2007), Reddy et al. (2020), Bondarev and Upmann (2022) for a rigorous treatment):

1. All regimes of the associated (2) have only regular steady-states. Resulting optimal trajectory never touches the Σ manifold and is obtained via conventional Maximum Principle

2. Some steady-states are virtual and some are regular. Depending on initial conditions, optimal trajectory may either cross or not the Σ. It is obtained via *hybrid* maximum principle as in Boltyanski (2004) or Shaikh and Caines (2007)

3. All steady-states are virtual, but the sliding region SL is non-empty. Both conventional and hybrid maximum principle are not applicable. We then use a modified version from Bondarev and Upmann (2022) to obtain the solution converging to the sliding equilibrium (pseudo-equilibrium). This is the main focus of our paper.

4. All steady-states are virtual and sliding region is empty. Possibility of crossing limit cycles as in Islas et al. (2021). This option is intended for future research.

4 Scenario I: Jump in albedo

In this scenario we assume that the albedo, function $\alpha_1(T)$, is piecewise constant:

$$\alpha_1(T) = \begin{cases} \alpha_1^U, T < T_s, \\ \alpha_1^L, T > T_s \end{cases} \tag{6}$$

In our experiment we assume the following benchmarks, $\alpha_1^U = 0.79$ and $\alpha_1^L = 0.78$, leaving T_s free for now. The specification (6) implies that the model (1) has two smooth regimes associated with α_1^U, α_1^L, respectively. In both regimes the triple of ODEs (1) has some special structure allowing us to deal with $\dot{T}$ equation only.

The equation of interest after substitution of all parameters is:

$$\frac{d}{dt}T(t) = 1612.200651 - 2283.734135\alpha_1(T) - 6.932304977 \times 10^{-8}T(t)^4 + \\ +32.40480962\ln(1.99039 - 0.9904\mathrm{e}^{-\frac{t}{10}}) \qquad (7)$$

Lemma 1. *The model* (1) *with jump in albedo as* (6) *has two steady-state values for* (7)*:* $\bar{T}_-, \bar{T}_+$ *of* $T(t)$ *given by the time-invariant part of equation* (7) *for* α_1^U, α_1^L*, respectively. In particular, we have* $\bar{T}_- < \bar{T}_+$ *as long as* $\alpha_1^U > \alpha_1^L$*.*

Proof. The steady-state for non-autonomous ODE is found in two steps. First the time-dependent part has to be a contraction in time. In case of (7) it is trivially so, since function $\mathrm{e}^{-\frac{t}{10}}$ decreases with time to zero. Second, the steady-state value of the time-invariant part is found. In our case this amounts to solving equation type $c_1^{\pm} - c_2\bar{T}_{\pm}^4 = 0$ for both regimes.

$$\bar{T}_{\pm} \overset{\frac{c_1^{\pm}}{c_2}>0}{=} \left(\frac{c_1^{\pm}}{c_2}\right)^{\frac{1}{4}} \qquad (8)$$

which proves first claim.

Second claim follows from the fact that by construction $\alpha_1^U > \alpha_1^L$ implies $c_1^- < c_1^+$ following from (8) $\bar{T}_- < \bar{T}_+$. □

In particular, for our parameter setting as in Table 1, we have $\bar{T}_- = 291.697 < \bar{T}_+ = 294.96$, close to the values obtained in the benchmark model. Both equilibria are stable for the 1-dimensional ODE (7). The overall 3-d system (1) is saddle-point stable as can be seen from the analysis of respective Jacobian matrices and, thus, can be reached by optimal trajectories (if they are regular ones) since $c(0)$ is free.

Now take into account that T_s is not fixed. We have three different configurations:

1. $T_s < \bar{T}_- < \bar{T}_+$. Only the steady-state of the upper regime with $\bar{T} = \bar{T}_+$ is regular. It is thus the unique steady-state of the overall system. The solution is obtained either via conventional maximum principle if $T_0 > T_s$[3] or through hybrid one if $T_0 < T_s$;

[3]by T_0 we understand initial condition for (7) above and other varieties below, technically meaning initial condition for a given initial value problem

2. $\bar{T}_- < T_s < \bar{T}_+$. Both steady-states are regular and can be reached: once $T_0 < T_s$, steady-state with $\bar{T}_-$ realises, once $T_0 > T_s$, steady-state with $\bar{T}_+$ realises;

3. $\bar{T}_- < \bar{T}_+ < T_s$. Only steady-state with $\bar{T} = \bar{T}_-$ is regular and is reached by the optimal trajectory, found as in point 1 above.

The most interesting and natural case is case 2, on which we focus further on. Apart from two long-run values $\bar{T}_\pm$ there is an opportunity for special dynamics around the *switching manifold* Σ which is defined by $T = T_s$. This manifold[4] partition into crossing, escaping and sliding regions follows Def. 2. In particular, because of the special structure of Σ (it depends on T only) we have:

$$\begin{aligned}\mathcal{L}_{f_+}(\mathbf{x})\alpha &= 502.421510 - 6.932304977 \times 10^{-8} T_s^4 + 32.40480962 \ln(M),\\ \mathcal{L}_{f_-}(\mathbf{x})\alpha &= 479.584168 - 6.932304977 \times 10^{-8} T_s^4 + 32.40480962 \ln(M)\end{aligned} \tag{9}$$

which are tangent lines separating Σ in three regions[5], two of which are *crossing* regions and one is *sliding/escaping*, depending on signs of derivatives as given in Def. 2.

Denote with $M^*_\pm :\ \mathcal{L}_{f_\pm}(\mathbf{x})\alpha = 0$ tangent lines of upper and lower vector fields. These, according to (9) are vertical lines in the $(M - c)$ plane at some particular values of $M^*_\pm$ being roots of above equations (for any T_s).

We can observe that for the parameter values chosen above the sliding region is always empty and the escaping is not, providing lemma 2.

Lemma 2. *For the jump regime* (6) *of the albedo in the model* (1) *the switching manifold* $\Sigma :\ T = T_s$ *has the following partition:*

1. *Crossing region* CR_1 *with crossing from upper regime to the lower for* $M \in [0, M^*_+]$

2. *Escaping region* ES *where trajectories cannot switch from one regime to another for* $M \in (M^*_+, M^*_-)$

3. *Crossing region* CR_2 *with crossing from lower regime to the upper for* $M \in [M^*_-, \infty)$

[4]Which is the hyperplane in the $(M - c)$ space for fixed T in our case.

[5]They do not intersect, so the general two-fold position is not possible in this case.

Sliding region is empty and no pseudo-equilibrium exists.

Proof. We start with observing that $M_+^* < M_-^*$ for any $T_s \geq 0$. Indeed, for any T_s fixed, we have $\mathcal{L}_{f_+}(M)\alpha > \mathcal{L}_{f_-}(M)\alpha$ as they are monotonic functions of M. It then follows that $\mathcal{L}_{f_+}(M)\alpha$ intersects zero at a lower M than $\mathcal{L}_{f_-}(M)\alpha$, see Figure 1.

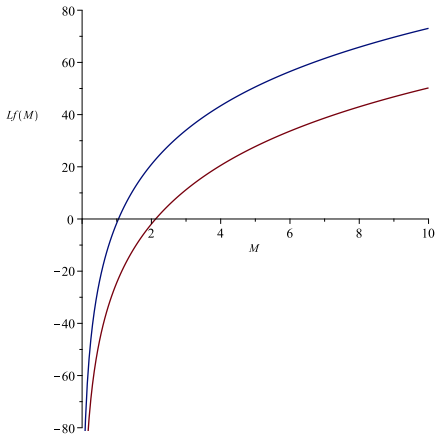

Figure 1: Functions $\mathcal{L}_{f_+}(M)\alpha$ (blue), $\mathcal{L}_{f_-}(M)\alpha$ (brown) showing $M_+^* < M_-^*$ for $T_s = 293$.

It next follows via Def. 2 that the region where both $\mathcal{L}_{f_+}(M)\alpha$, $\mathcal{L}_{f_-}(M)\alpha$ are negative is constrained by M_+^* from above. This is the region where dynamics in both regimes is going "down" in terms of T, making crossing region CR_1.

Further, for $M \in (M_+^*, M_-^*)$ we have $\mathcal{L}_{f_+}(M)\alpha > 0$ but $\mathcal{L}_{f_-}(M)\alpha < 0$ which defines the escaping region.

At last, for $M > M_-^*$ both $\mathcal{L}_{f_\pm}(M)\alpha > 0$ defining crossing region CR_2 where both regimes have dynamics pointing into higher values of T.

Since this last region is not constrained from above, it also follows that $SL = \emptyset$ which concludes the proof. □

The topology of Σ is given by Figure 2.

We conclude with a summary of possible long-run outcomes in the system (1) with the albedo modelled as in (6).

Proposition 1. *The model* (1) *with a non-smooth jump in the albedo as in* (6) *has the following properties:*

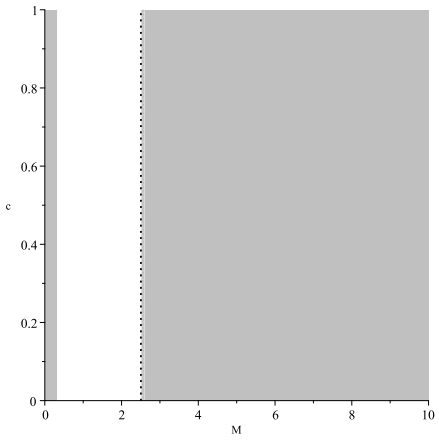

Figure 2: Partition of $\Sigma: \ T = T_s$ for jump in albedo. Grey areas are crossing regions, white is escaping region. T_s set to $293K$.

1. *There exist two long-run steady-states* $\bar{x}_+ := \{\bar{T}_+, \bar{c}_+, \ \bar{M}_+\}, \bar{x}_- := \{\bar{T}_-, \bar{c}_-, \bar{M}_-\}$ *such that* $\bar{T}_- < \bar{T}_+, \ \bar{M}_- = \bar{M}_+, \ \bar{c}_+ < \bar{c}_-$

2. *Once* $T_s < \bar{T}_-$*, only* $\bar{x}_+$ *is regular and feasible, it is the only unique optimal long-run steady-state*

3. *Once* $T_s > \bar{T}_+$*, only* $\bar{x}_-$ *is regular and feasible, it is the only unique optimal long-run steady-state*

4. *Once* $\bar{T}_+ > T_s > \bar{T}_-$ *both steady-states may realise depending on* $T_0 \gtreqless T_s$*. Additionally, crossing limit cycles may be present and optimal.*

Proof. Claims 1-3 follows from Lemma 1. Claim 4 follows from Lemma 2 □

Overall, except for the potential of crossing limit cycles (yet to be studied), the model with a jump in the albedo provides predictions very close to the benchmark smoothed model. We now make the next step and assume that the albedo is described by a non-smooth linearly decreasing function.

5 Scenario II: Linear trend in albedo

In this case we follow the original formulation of the albedo function as in the benchmark paper with:

$$\alpha_2(T) = \begin{cases} \alpha_2^U, T < T_l, \\ \alpha_2^U - k_T(T - T_l),\ T_u > T > T_1, \\ \alpha_2^L, T > T_u \end{cases} \tag{10}$$

where we assume $\alpha_2^U = \alpha_1^U$ and $\alpha_2^L = \alpha_1^L$ from above.
Applying this to the model (1) we find that around the first switching point with $T = T_l$ only the escaping region is non-empty while the sliding one is.

Next, we proceed in the same way as above identifying steady-state values for T, analyzing the structure of switching manifolds and, finally, characterizing the global dynamical picture.

First, note that under scenario (10) the system (1) has *three* regimes. Two of them are the same as in the previous section, and the transitory regime with a linear decrease in albedo is the novel one. We observe that this transitory regime (denoted by $f_L := \{\dot{T}_L, \dot{M}_L, \dot{c}_L\}$ to distinguish from $f_\pm$) has its own steady-state with temperature steady state value denoted by $\bar{T}_L : \dot{T}_L = 0$.

We thus have to study two switchings in turn[6], which we do in the following.

5.1 First switching at T_l

At the first switching threshold (denoted by $\Sigma_- :\ T = T_l$) the lower vector field $f_-(\mathbf{x})$ is the same as in the scenario with albedo jump, but the upper vector field is different as it has the linearly decreasing trend in the albedo.

Repeating the arguments from the previous section we can characterize the switching manifold $T = T_l$ via two tangent lines:

$$\begin{aligned} \mathcal{L}_{f_L}(\mathbf{x})\alpha &= -2808.992986 + 11.41867068T_l - 6.932304977 \times 10^{-8}T_l^4 + 32.40480962\ln(M), \\ \mathcal{L}_{f_-}(\mathbf{x})\alpha &= 479.584168 - 6.932304977 \times 10^{-8}T_l^4 + 32.40480962\ln(M) \end{aligned} \tag{11}$$

[6] assuming time is only positive, $t \in \mathbb{R}_{>0}$

We can define

$$T_l^* : \ \mathcal{L}_{f_L}(\mathbf{x})\alpha = \mathcal{L}_{f_-}(\mathbf{x})\alpha \tag{12}$$

as the temperature threshold such that both tangent lines coincide for that temperature.[7] Further, denote as above $M_-^* : \ \mathcal{L}_{f_-}(\mathbf{x})\alpha = 0$, $M_L^* : \ \mathcal{L}_{f_L}(\mathbf{x})\alpha = 0$, being M values where both tangent lines (being vertical lines in Σ_- plane) are located.

It then follows from (11), that

$$\forall 0 \geq T_l < T_l^* : \ \mathcal{L}_{f_L}(\mathbf{x})\alpha < \mathcal{L}_{f_-}(\mathbf{x})\alpha, \tag{13}$$

$$\forall T_l > T_l^* : \ \mathcal{L}_{f_L}(\mathbf{x})\alpha > \mathcal{L}_{f_-}(\mathbf{x})\alpha \tag{14}$$

Then, given the parameters chosen, the switching manifold Σ_- has three regions only, two crossing ones and the sliding/escaping one depending on the location of T_l:

Lemma 3. *For the linear trend regime* (10) *of albedo in the model* (1) *the first switching manifold* $\Sigma_- : \ T = T_l$ *has the following partition:*

1. *For* $T_l > T_l^*$*:*

   (a) *Crossing region* CR_1 *with crossing from upper regime* f_L *into the lower one* f_- *for* $M \in [0, M_L^*]$,

   (b) *Escaping region* ES *for* $M \in [M_L^*, M_-^*]$

   (c) *Crossing region* CR_2 *with crossing from lower regime* f_- *into upper* f_L *for* $M \in [M_-^*, \infty)$

   (d) *Sliding region is empty and no pseudo-equilibrium may realise.*

2. *For* $T_l < T_l^*$*:*

   (a) *Crossing region* CR_1 *with crossing from lower regime* f_- *into the upper one* f_L *for* $M \in [0, M_-^*]$,

   (b) *Sliding region* SL *for* $M \in [M_-^*, M_L^*]$

[7] For our parameter setting this equals $T_l^* = 288K$.

(c) *Crossing region CR_2 with crossing from upper regime f_L into lower f_- for $M \in [M_L^*, \infty)$*

(d) *Escaping region is empty and no crossing limit cycles may realise.*

Proof. Proof is fully equivalent to the proof of lemma 2 with additional observation that $\mathcal{L}_{f_L}(\mathbf{x})\alpha$ has a linear term in T and, thus, can be both lower or higher than $\mathcal{L}_{f_-}(\mathbf{x})\alpha$. Figure 3 illustrates the situation. □

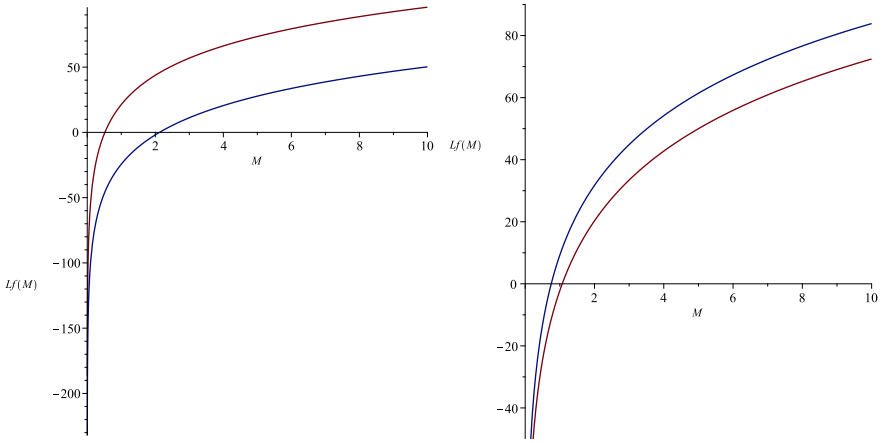

(a) $M_L^* < M_-^*$ for $T_l^* < T_l = 292K$. (b) $M_-^* < M_L^*$ for $T_l^* > T_l = 287K$.

Figure 3: Functions $\mathcal{L}_{f_-}(M)\alpha$ (blue) and $\mathcal{L}_{f_L}(M)\alpha$ (brown) for cases $T_l > T_l^*$ (left) and $T_l < T_l^*$ (right)

For realistic temperature settings Figure 4 shows that the sliding region cannot realise, since $T_l^* < T_0 = 288K$.

Hence, the lower regime is identical to the one from the previous section and has the same steady-state characterization (see lemma 1), but, the transitory regime T_L has *two* different steady-states, $\bar{T}_L^i$, $i = 1, 2$. We postpone the global steady-states analysis to later, first studying the switching manifold structure around the second switching point, $\Sigma_+ : \ T = T_u > T_l$.

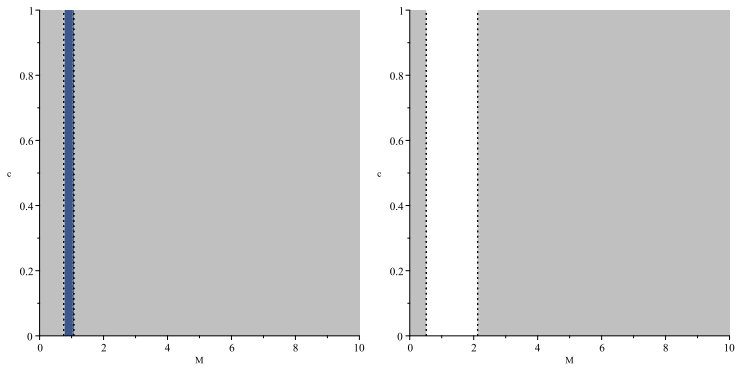

(a) Non-empty sliding region for $T_l = 287 < T_l^*$

(b) Non-empty escaping region for $T_l = 292 > T_l^*$

Figure 4: Partition of Σ_- : $T = T_l$ for albedo model (10). Grey areas are crossing regions, blue area is the sliding region.

5.2 Second switch at $T = T_u$

Around the second switching point $T = T_u$, on the contrary, the escaping region is empty but the sliding region is not. According to Bondarev and Upmann (2022) we could expect the sliding pseudo-equilibrium to be the long-run optimal outcome once conventional steady-states are virtual.

The structure of Σ_+ is defined by two tangent lines:

$$\begin{aligned}\mathcal{L}_{f_L}(\mathbf{x})\alpha &= -2808.992986 + 11.41867068T_l - 6.932304977 \times 10^{-8}T_l^4 + 32.40480962\ln(M),\\ \mathcal{L}_{f_+}(\mathbf{x})\alpha &= 502.421510 - 6.932304977 \times 10^{-8}T_s^4 + 32.40480962\ln(M),\end{aligned} \tag{15}$$

where again $\mathcal{L}_{f_+}(\mathbf{x})\alpha$ is the same as for the upper regime in the albedo jump scenario and $\mathcal{L}_{f_L}(\mathbf{x})\alpha$ is the tangent line of the vector field characterizing the intermittent regime with the linear albedo increase. We define T_u^* : $\mathcal{L}_{f_L}(\mathbf{x})\alpha = \mathcal{L}_{f_+}(\mathbf{x})\alpha$ and observe that as above, M_+^* : $\mathcal{L}_{f_+}(\mathbf{x})\alpha = 0$, M_L^* : $\mathcal{L}_{f_L}(\mathbf{x})\alpha = 0$, being M values where both tangent lines (being vertical lines in Σ_+ plane) are located.

We first observe that for our parameter values we have $T_u^* = 290K$. Thus, we obtain $M_+^* < M_L^*$ for $T_u > T_u^*$ and vice versa.

$$\forall 0 \geq T_u < T_u^* : \ 0 < \mathcal{L}_{f_L}(\mathbf{x})\alpha < \mathcal{L}_{f_-}(\mathbf{x})\alpha, \ M_+^* < M_L^* \tag{16}$$

$$\forall T_u > T_u^* : \ \mathcal{L}_{f_L}(\mathbf{x})\alpha > \mathcal{L}_{f_-}(\mathbf{x})\alpha, \ M_+^* > M_L^* \tag{17}$$

We recover the counterpart of lemma 3:

Lemma 4. *For the linear trend regime* (10) *of albedo in the model* (1) *the second switching manifold* $\Sigma_+ : \ T = T_u$ *has the following partition:*

1. *For* $T_u > T_u^*$*:*
   (a) *Crossing region* CR_1 *with crossing from upper regime* f_+ *into the lower one* f_L *for* $M \in [0, M_L^*]$,
   (b) *Sliding region* SL *for* $M \in [M_L^*, M_+^*]$
   (c) *Crossing region* CR_2 *with crossing from lower regime* f_L *into upper* f_+ *for* $M \in [M_+^*, \infty)$
   (d) *Escaping region is empty and no crossing limit cycles may realise.*
2. *For* $T_u < T_u^*$*:*
   (a) *Crossing region* CR_1 *with crossing from lower regime* f_L *into the upper one* f_+ *for* $M \in [0, M_+^*]$,
   (b) *Escaping region* ES *for* $M \in [M_+^*, M_L^*]$
   (c) *Crossing region* CR_2 *with crossing from upper regime* f_+ *into lower* f_L *for* $M \in [M_L^*, \infty)$
   (d) *Sliding region is empty and no pseudo-equilibrium may realise.*

Proof. Fully equivalent to lemmata 2, 3 □

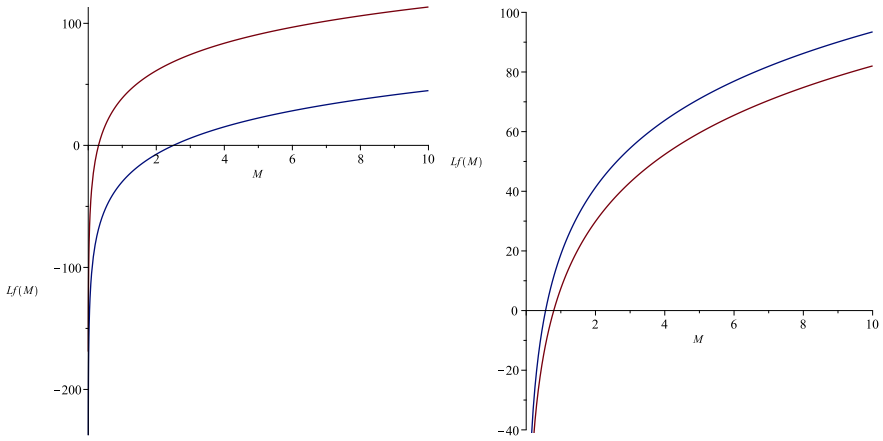

(a) $M_L^* < M_+^*$ for $T_u^* < T_u = 296K$. (b) $M_+^* < M_L^*$ for $T_u^* > T_u = 289K$.

Figure 5: Functions $\mathcal{L}_{f_+}(M)\alpha$ (blue) and $\mathcal{L}_{f_L}(M)\alpha$ (brown) for cases $T_u > T_u^*$ (left) and $T_u < T_u^*$ (right)

Figure 6 shows two potential cases for the partition of Σ_+. We note that for our parameter values $T_u^* = 290$, so it is more likely that $T_u > T_u^*$ than otherwise.[8]

Thus, we focus the global steady-state analysis for the albedo model (10) on the case where $T_l > T_l^*$, $T_u > T_u^*$ holds, i.e. the sliding region is non-empty only for the upper switching threshold, but not for the lower one.

5.3 Global steady-states analysis

For the chosen parameter values it turns out that the following holds true.

Lemma 5. *The model* (1) *with trend in albedo* (10) *has two steady-states* $\bar{T}_- < \bar{T}_+$ *for* $\alpha_2^U > \alpha_2^L$ *coinciding with those from lemma 1 and two additional steady-states* $\bar{T^1}_L < \bar{T^2}_L$.

For the chosen parameter settings it holds that $\bar{T^1}_L < \bar{T}_- < \bar{T}_+ < \bar{T^2}_L$.

We cannot give a general proof of this lemma. The result in the lemma was obtained by numerical computations and follows from comparing the roots of quartic equations.

[8]With the convention $T(0) = 288K$ and the current value of about 289K, it seems logical to set $T_u > 290K$ since there is no trend in the outgoing longwave radiation emitted to space over the last 50 years despite the increasing temperature, see https://www.ncei.noaa.gov/access/monitoring/enso/olr

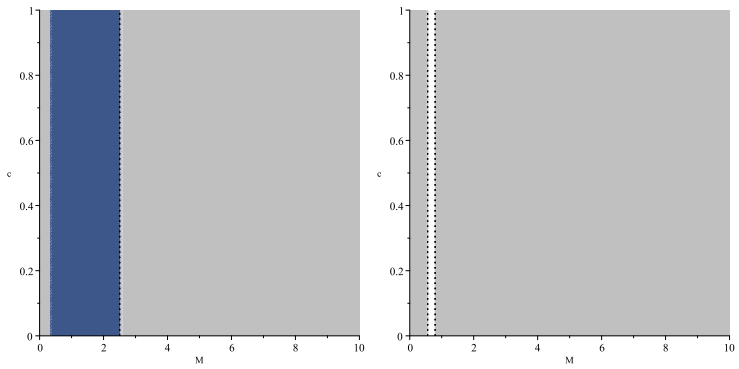

(a) Non-empty sliding region for $T_u = 296 > T_u^*$

(b) Non-empty escaping region for $T_u = 289 < T_u^*$

Figure 6: Partition of Σ_+ : $T = T_u$ for albedo model (10). Grey areas are crossing regions, blue area is the sliding region.

Thus, we need to investigate under which conditions all steady-states are regular/virtual. This, in turn, depends on the values of T_l, T_u. In Sec. 4 we argued that $\bar{T}_- < T_s < \bar{T}_+$ is the most likely case. Positing that $T_l < T_s < T_u$ we can have the following configurations:

1. $\bar{T}_L^1 < T_l < \bar{T}_- < \bar{T}_+ < T_u < \bar{T}_L^2$: All normal steady-states are virtual. Only sliding equilibrium at $T = T_u$ can be the optimal outcome.
2. $T_l < \bar{T}_L^1 < \bar{T}_- < \bar{T}_+ < T_u < \bar{T}_L^2$: Only $\bar{T}_L^1$ is regular.
3. $T_l < \bar{T}_L^1 < \bar{T}_- < \bar{T}_+ < \bar{T}_L^2 < T_u$: both $\bar{T}_L^{1,2}$ are regular.
4. $\bar{T^1}_L < \bar{T}_- < T_l < T_u < \bar{T}_+ < \bar{T^2}_L$: both $\bar{T}_\pm$ are regular.
5. $\bar{T^1}_L < T_l < \bar{T}_- < T_u < \bar{T}_+ < \bar{T^2}_L$: only $\bar{T}_+$ is regular.
6. $\bar{T^1}_L < \bar{T}_- < T_l < \bar{T}_+ < T_u < \bar{T^2}_L$: only $\bar{T}_-$ is regular.

We now will try to sort out some of outcomes as not fitting our parameters. First, observe that for our values, $\bar{T}_L^1 = 287.44K$, $\bar{T}_L^2 = 397.36K$, so surely we have $\bar{T}_L^1 < T_l < T_u < \bar{T}_L^2$. This sorts out cases 2,3 above.

Second, following the observations above we set $T_l > T_l^* = 288K$, $T_u > T_u^* = 290K$. For our parameters we have $\bar{T}_- = 288.4K$, $\bar{T}_+ = 291.77K$ so cases 4-6 may realise only for

the relatively narrow range of $T_u \in [290K, 291.4K]$, $T_l \in [288.5K, 290K]$, otherwise case 1 realises. We do not stop to discuss which range is more likely to realise, but notice that cases 4-6 are qualitatively equivalent to those studied in the benchmark model (albeit with slightly different steady-state values). Instead, we focus on the case 1 as the qualitatively novel one. We summarise our discussion in the following corollary.

Corollary 1. *For the chosen parameter values the configuration* $\bar{T}_L^1 < T_l < \bar{T}_- < \bar{T}_+ < T_u < \bar{T}_L^2$ *is generic and implies the sliding equilibrium as the only optimal outcome.*

5.4 Sliding flow for model (10).

According to the general theory (Sec. 3) the sliding flow via Filippov's method at the switching manifold $\Sigma_+ : \ T = T_u$ is given as follows:

$$\begin{aligned} \dot{M} &= 0.19904 - 0.1M(t), \\ \dot{c} &= -0.0096 - \frac{0.1636}{(0.04(T_u - T_0)^2 + 1)^{0.05} + c(t)} \end{aligned} \tag{18}$$

It has two equilibria: $\bar{x}_l^1 := \{T_u, \bar{M}_l, 0\}$, $\bar{x}_l^2 := \{T_u, \bar{M}_l, \bar{c}_l\}$ that differ only in consumption per capita with one of them implying *zero consumption*. The analysis of the Jacobian matrix demonstrates that the equilibrium with zero consumption is the only stable one and the other is unstable. Thus, it becomes evident that under the configuration of Corr. 1, it inevitably will undergo the collapse in consumption going to zero once the overall economy enters the sliding mode. Figure 7 illustrate the outcome with the help of the phase diagram.

The steady-state associated with a long-run consumption level of zero yields a smaller utility functional than the steady-state with a strictly positive level of consumption. Thus, the steady-state with a zero long-run consumption level cannot be optimal because the goal of the representative individual is to maximize the discounted stream of utilities resulting from consumption. Hence, $\bar{x}_l^2$ is the optimal solution which can be proven if we use the result of the modified maximum principle from Bondarev and Upmann (2022). We can state the following proposition.

Proposition 2. *For the competitive economy* (1) *under linear albedo change* (10) *with* $\bar{T}_L^1 < T_l < \bar{T}_- < \bar{T}_+ < T_u < \bar{T}_L^2$ *the only optimal outcome is the trajectory* $\mathbf{x}(t) :=$

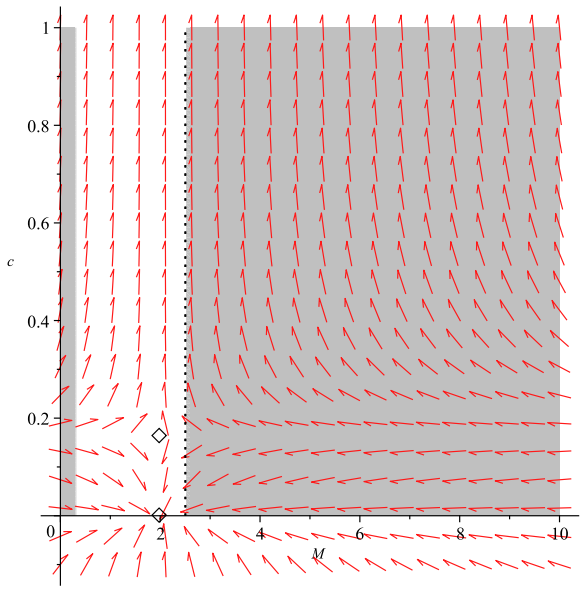

Figure 7: Phase diagram of sliding flow vector field (red arrows) with regions $CR_{1,2}$ greyed out. Points mark two pseudo-equilibria: the trivial and the non-trivial one.

$\{T(t), M(t), c(t)\}$ *converging to the non-degenerate pseudo-equilibrium* $\bar{x}_l^2$ *implying long-run stabilization of the temperature at* $T = T_u$ *and a non-zero consumption level.*

Proof. Using the result of the aforementioned paper we note that the pseudo-equilibrium may be optimal if two conditions hold:

- All normal steady-states are virtual: this is provided by assumption $\bar{T}_L^1 < T_l < \bar{T}_- < \bar{T}_+ < T_u < \bar{T}_L^2$.
- The pseudo-equilibrium itself is *weakly feasible*[9] which is due to the fact that $\bar{x}_l^2$ is unstable within the sliding flow.

□

It should be noted that the pseudo-equilibrium with the value $T = T_u$ can be reached although that equilibrium is unstable in Σ. This holds because the sliding region is non-empty so that there exists a set with non-zero measure of trajectories leading to any point

[9]In Bondarev and Upmann (2022) weak feasibility is defined as the topological property of a point at Σ such that it can be reached only from outside of Σ in a unique way for any $\mathbf{x}(0)$.

of the sliding region from the outside. These trajectories are all continuous: one just has to select the starting value $c(0)$ such that the trajectory converges to the fixed endpoint $\bar{c}$ of the pseudo-equilibrium, i.e. such that $\lim_{t\to\infty} c(t) = \bar{c}$ holds.

6 Conclusion

Low-dimensional climate models describe the time path of the average global surface temperature as a function of the temperature and of the stock of GHGs, given predetermined parameter values. However, with an increasing temperature on earth, the parameter values can change, too, thus giving rise to so-called feedback effects. Feedback effects may occur suddenly, best described by a discontinuous jump of a parameter, or it may take some time until the new parameter value is achieved with the transition period characterized by a continuous function with kinks at the upper and lower boundary. Hence, models where the change is described by a smooth, i.e. differentiable, function are just an approximation of the non-smooth one that comes closer to the real world.

In this paper we made use of the model by Greiner and Semmler (2005) as a starting point, where a changing albedo was approximated by a smooth function, to show how non-smooth changes in the parameters of the underlying system may alter the results of modelling and related policy implications. For the model with a discontinuous jump in the albedo, we found that multiple regular steady-states may occur when the switching point is located between the lower and the upper steady-state temperature. This result is qualitatively the same as the one in the benchmark model. A new additional result we could derive is that the steady-state is unique if the switching point is either below or above the two regular steady-state temperatures.

When the albedo is described by a piecewise smooth function more complex dynamics may result. On the one hand, we again observe that there are parameter constellations such that the results of the benchmark model are replicated from a qualitative point of view. But, on the other hand we could show that all steady-states are virtual and that a non-degenerate pseudo-equilibrium exists, where the temperature stabilizes exactly at the upper switching level of the albedo with a strictly positive level of consumption.

Overall, we can conclude that allowing for a non-smooth variation of the albedo of the earth leads to richer dynamics compared to the model where the albedo is approximated by a differentiable function. This holds because there exist additional long-run equilibria besides those that are obtained for the model where a smooth function describes the change in the albedo.

With respect to policy implications, things do not become easier, but, more complicated. This is simply due to the fact that more constellations are possible that policy makers must take into account. To give precise policy recommendations, a more detailed knowledge of the climate system would be necessary that, however, is difficult to obtain. Nevertheless, even if our model is a low-dimensional and a very stylized one, a conclusion we can draw is that a decline in the temperature as a result of decreasing GHG emissions is feasible. This holds because the pseudo-equilibrium can be reached only from outside of the sliding region and, consequently, from a temperature exceeding the upper threshold. That result counters in a way the fatalistic argument that it would be impossible to revert global warming, once a certain threshold of the temperature is passed, although it should be kept in mind that our approach is a highly stylized one.

References

Alimonti, G. and L. Mariani (2023). Is the number of global natural disasters increasing? *Environmental Hazards*, doi: 10.1080/17477891.2023.2239807.

Boltyanski, V. (2004). The maximum principle for variable structure systems. *International Journal of Control 77*(17), 1445–1451.

Bondarev, A. and T. Upmann (2022). Sliding modes in the management of renewable resources. *Automatica 144*, 110487.

Chen, D., M. Rojas, B. Samset, K. Cobb, A. Diongue Niang, P. Edwards, S. Emori, S. Faria, E. Hawkins, P. Hope, P. Huybrechts, M. Meinshausen, S. Mustafa, G.-K. Plattner, and A.-M. Tréguier (2021). Framing, context, and methods. In V. Masson-Delmotte, P. Zhai, A. Pirani, S. Connors, C. Pean, S. Berger, N. Caud, Y. Chen,

L. Goldfarb, M. Gomis, M. Huang, K. Leitzell, E. Lonnoy, J. Matthews, T. Maycock, T. Waterfield, O. Yelekci, R. Yu, and B. Zhou (Eds.), *Climate Change 2021: The Physical Science Basis. Contribution of Working Group I to the Sixth Assessment Report of the Intergovernmental Panel on Climate Change*, pp. 147–286, doi:10.1017/9781009157896.003. Cambridge, New York: Cambridge University Press.

Colombo, A. and M. R. Jeffrey (2011). Nondeterministic chaos, and the two-fold singularity in piecewise smooth flows. *SIAM Journal on Applied Dynamical Systems 10*(2), 423–451.

Di Bernardo, M., C. Budd, A. Champneys, P. Kowalczyk, A. Nordmark, G. Olivar, and P. Piiroinen (2008). Bifurcations in nonsmooth dynamical systems. *SIAM Review 50*(4), 629–701.

Etminan, M., G. Myhre, E. Highwood, and K. Shine (2016). Radiative forcing of carbon dioxide, methane, and nitrous oxide: a significant revision of the methane radiative forcing. *Geophysical Research Letters 43*, 12,614–12,623, https://doi.org/10.1002/2016GL071930.

Greiner, A., B. Bökemeier, and B. Owusu (2023). Climate change and economic growth: Evidence for european countries. *Bielefeld University, Working Papers in Economics and Management, No. 07-2023*, http://dx.doi.org/10.2139/ssrn.4626705.

Greiner, A. and W. Semmler (2005). Economic growth and global warming: A model of multiple equilibria and thresholds. *Journal of Economic Behavior and Organization 57*, 430–447.

Greiner, A. and W. Semmler (2008). *The Global Environment, Natural Resources, and Economic Growth.* Oxford, New York: Oxford University Press.

Henderson-Sellers, A. and K. McGuffie (1987). *A Climate Modelling Primer.* Chichester: Wiley.

Islas, J. M., J. Castillo, B. Aguirre-Hernandez, and F. Verduzco (2021). Pseudo–Hopf Bifurcation for a Class of 3D Filippov Linear Systems. *International Journal of Bifurcation and Chaos 31*(2), 2150025–1840.

Jacquemard, A., M. A. Teixeira, and D. J. Tonon (2013). Stability conditions in piecewise smooth dynamical systems at a two-fold singularity. *Journal of Dynamical and Control Systems 19*(1), 47–67.

Lee, J.-Y., J. Marotzke, G. Bala, L. Cao, S. Corti, J. Dunne, F. Engelbrecht, E. Fischer, J. Fyfe, C. Jones, A. Maycock, J. Mutemi, O. Ndiaye, S. Panickal, and T. Zhou (2021). 'future global climate: Scenario-based projections and near term information. In V. Masson-Delmotte, P. Zhai, A. Pirani, S. Connors, C. Pean, S. Berger, N. Caud, Y. Chen, L. Goldfarb, M. Gomis, M. Huang, K. Leitzell, E. Lonnoy, J. Matthews, T. Maycock, T. Waterfield, O. Yelekci, R. Yu, and B. Zhou (Eds.), *Climate Change 2021: The Physical Science Basis. Contribution of Working Group I to the Sixth Assessment Report of the Intergovernmental Panel on Climate Change*, pp. 553–672, doi:10.1017/9781009157896.006. Cambridge, New York: Cambridge University Press.

Lomborg, B. (2020). Welfare in the 21st century: increasing development, reducing inequality, the impact of climate change, and the cost of climate policies. *Technological Forecasting & Social Change 156*, 119981.

Piecuch, C. and L. Beal (2023). Robust weakening of the gulf stream during the past four decades observed in the florida straits. *Geophysical Research Letters 50*, e2023GL105170. https://doi.org/10.1029/2023GL105170.

Ranasinghe, R., A. Ruane, R. Vautard, N. Arnell, E. Coppola, F. Cruz, S. Dessai, A. Islam, M. Rahimi, D. Ruiz Carrascal, J. Sillmann, M. Sylla, C. Tebaldi, W. Wang, and R. Zaaboul (2021). Climate change information for regional impact and for risk assessment. In V. Masson-Delmotte, P. Zhai, A. Pirani, S. Connors, C. Pean, S. Berger, N. Caud, Y. Chen, L. Goldfarb, M. Gomis, M. Huang, K. Leitzell, E. Lonnoy, J. Matthews, T. Maycock, T. Waterfield, O. Yelekci, R. Yu, and B. Zhou (Eds.), *Climate Change 2021: The Physical Science Basis. Contribution of Working Group I*

to the Sixth Assessment Report of the Intergovernmental Panel on Climate Change, pp. 1767–1926, doi:10.1017/9781009157896.014. Cambridge, New York: Cambridge University Press.

Reddy, P. V., J. M. Schumacher, and J. Engwerda (2020). Analysis of optimal control problems for hybrid systems with one state variable. *SIAM Journal on Control and Optimisation 58*(6), 3262–3292.

Schmitz, G. (1991). Klimatheorie und -modellierung. In P. Hupfer (Ed.), *Das Klimasystem der Erde: Diagnose und Modellierung, Schwankungen und Wirkungen*, pp. 181–217. Berlin: Akademie Verlag.

Shaikh, M. S. and P. E. Caines (2007). On the hybrid optimal control problem: Theory and algorithms. *IEEE Transactions on Automatic Control 52*(9), 1587–1603.

Tang, S., J. Liang, Y. Xiao, and R. A. Cheke (2012). Sliding bifurcations of Filippov two stage pest control models with economic thresholds. *SIAM Journal on Applied Mathematics 72*(4), 1061–1080.